

Effective Field Theory for Layered Quantum Antiferromagnets with Non-Magnetic Impurities

Yu-Chang Chen and A. H. Castro Neto

Department of Physics, University of California, Riverside, CA, 92521

(July 6, 2017)

We propose an effective two-dimensional quantum non-linear sigma model combined with classical percolation theory to study the magnetic properties of site diluted layered quantum antiferromagnets like $\text{La}_2\text{Cu}_{1-x}\text{M}_x\text{O}_4$ ($\text{M}=\text{Zn}, \text{Mg}$). We calculate the staggered magnetization at zero temperature, $M_s(x)$, the magnetic correlation length, $\xi(x, T)$, the NMR relaxation rate, $1/T_1(x, T)$, and the Néel temperature, $T_N(x)$, in the renormalized classical regime. Due to quantum fluctuations we find a quantum critical point (QCP) at $x_c \approx 0.305$ at lower doping than the two-dimensional percolation threshold $x_p \approx 0.41$. We compare our results with the available experimental data.

PACS numbers: 75.10.-b, 75.10.Jm, 75.10.Nr

The discovery of high temperature superconductivity in $\text{La}_{2-x}\text{Sr}_x\text{CuO}_4$ has motivated an enormous number of experimental and theoretical studies of this and related materials. La_2CuO_4 has attracted a lot of interest because it is a classical example of a quantum Heisenberg antiferromagnet (QHAF). La_2CuO_4 is a layered quasi-two-dimensional (2D) QHAF, with an intraplanar coupling constant J ($J/k_B \approx 1500$ K) much larger than the interplanar coupling J_\perp ($\approx 10^{-5}J$) [1]. The quantum nonlinear sigma model (QNL σ M) is probably the simplest continuum model with correct symmetry and spin-wave spectrum that reproduces the low-energy behavior of a QHAF. It has been successfully used [1] to explain many magnetic properties of $\text{La}_{2-x}\text{Sr}_x\text{CuO}_4$ [2].

In this paper we propose a QNL σ M allied to classical percolation theory to study the site dilution effect in $\text{La}_2\text{Cu}_{1-x}\text{M}_x\text{O}_4$, where M is a non-magnetic atom. While the theory of disordered classical magnetic systems is fairly developed [3] we still lack deep understanding of the behavior of the site diluted QHAF [4]. As we show below the interplay between quantum fluctuations and disorder leads to new effects which cannot be found in classical magnets. In particular we show that long-range order (LRO) is lost before the system reaches the classical percolation threshold. Furthermore, we have only two independent parameters in the theory: the spin-wave velocity c_0 (≈ 0.74 eV $\text{\AA}/\hbar$ [5]) and the bare coupling constant \bar{g}_0 (≈ 0.685 [1]) of the clean system ($x = 0$). The results for the staggered magnetization, correlation length, NMR relaxation rate and Néel temperature are derived without any further adjustable parameters.

Our starting point is the 2D site diluted nearest-neighbor isotropic Heisenberg model

$$H = J \sum_{\langle i, j \rangle} p(\mathbf{r}_i) p(\mathbf{r}_j) \mathbf{S}_i \cdot \mathbf{S}_j, \quad (1)$$

where $p(\mathbf{r})$ is the distribution function for Cu sites: $p(\mathbf{r}) = 1$ on Cu sites and $p(\mathbf{r}) = 0$ on M sites. Although translational invariance has been lost in (1), the Hamiltonian retains the $\text{SU}(2)$ invariance for rotations

in spin space. Since the symmetry is continuous Goldstone's theorem predicts the existence of a gapless mode in the broken symmetry phase. The ordered phase is characterized by a finite expectation value of the magnetization, $\mathbf{n} = \langle \mathbf{S}(\mathbf{Q}) \rangle$, at the antiferromagnetic ordering vector $\mathbf{Q} = (\pi/a_0, \pi/a_0)$ ($a_0 = 3.8$ \AA).

In the pure system, in accord with the Hohenberg-Mermin-Wagner theorem, LRO for a system with continuous symmetry is only possible at finite temperatures in dimensions larger than 2. In the absence of disorder the system has a Goldstone mode which is a spin wave around \mathbf{Q} with energy $E(\mathbf{k})$ and linear dispersion relation with the wave-vector \mathbf{k} : $E(\mathbf{k}) = \hbar c |\mathbf{k}|$, where c is the spin-wave velocity. This dispersion relation is a consequence of the Lorentz invariance of the system. In the paramagnetic phase, where the continuous symmetry is recovered, all excitations are gapped because order is only retained in a region of size ξ . In this case the excitations have dispersion

$$E(\mathbf{k}) = \hbar c \sqrt{\mathbf{k}^2 + 1/\xi^2}. \quad (2)$$

Now consider the case where quenched disorder is present. Spin-wave theory, which can only be applied to (1) at $T = 0$, predicts that Lorentz invariance is lost even for an infinitesimal amount of impurities [7]. The dispersion changes to $k \ln(k)$ and the spin waves become damped at a rate proportional to k when $k \rightarrow 0$. These results (strictly valid in 2D and $T = 0$) are not directly applicable to the systems in question which order at finite temperature [8]. At finite temperatures and weak disorder we can consider the criterion established by Harris for the relevance of disorder in critical phenomena [9]. Firstly, we can classify the phase diagram of the pure system as [1]: renormalized classical (RC) where $\xi(T)$ diverges as $\exp(T_0/T)$ (where T_0 is a characteristic temperature scale - see (6)); quantum critical (QC) where $\xi(T) \propto 1/T$; quantum disordered (QD) where $\xi(T) \approx \xi_0$ is constant. If we imagine the pure system being divided into regions of size ξ , each part will have fluctuations in the microscopic coupling constant (g , say) which by the central limit theorem are

proportional to the square root of the number of spins $N(\xi) \propto \xi^2$ in that region. That is, there are statistical fluctuations of order $\delta g(\xi) \propto 1/\sqrt{N(\xi)} \propto 1/\xi$. On the other hand the thermal fluctuations in the system are of order $\delta T(\xi) \propto 1/\ln(\xi/a_0)$ in RC, a_0/ξ in the QC and vanishingly small in the QD region. For the critical behavior of the system with weak disorder to be essentially the same as for the pure system one must require that $\delta T(\xi) \gg \delta g(\xi)$ when $\xi \gg a_0$. Observe that this condition is always fulfilled in the RC regime and therefore we expect the critical behavior to be the same as in the pure system, that is, described by a QNL σ M [1]. In the QC and QD regimes the situation is not clear because $\delta T(\xi) \sim \delta g(\xi)$ and therefore the effect of disorder is strong. We conjecture that in these regimes the critical behavior is different from the one described by a QNL σ M. In this work we focus entirely in the RC regime. Having these results in mind we can apply classical percolation theory to (1) [10,11]. The main parameters of the problem depend on geometrical factors such as the probability of finding a spin in the infinite cluster $P_\infty(x)$ ($\approx 1 - x$, for $x \ll 1$) and the bond dilution factor [12] $A(x)$ ($\approx 1 - \pi x + \pi x^2/2$) (in the expressions below $P_\infty(x)$ and $A(x)$ are valid for all x as given by the numerical simulations [11]). In the classical case the spin stiffness $\rho_s(x)$ is related to the undoped stiffness by $\rho_s(x) = A(x)\rho_s(0)$, while the transverse susceptibility is given by $\chi_\perp(x) = (P_\infty(x)/A(x))\chi_\perp(0)$ so that [13] $\rho_s(x) = c^2(x)\chi_\perp(x)$.

In this paper we propose an effective field theory which is valid for $T_N \leq T < J/k_B$ and combines the Lorentz invariance implied in (2), the Harris criterion and the results of percolation theory. In percolation theory, besides the infinite cluster, we always have finite clusters. A finite cluster of size L has discrete energy levels and therefore a gap of order $\hbar c/L$. In what follows we assume $\xi \gg L$ and ignore the contribution of finite clusters to the magnetic properties and focus entirely on the physics of the infinite cluster. It is obvious from the definition of $p(\mathbf{r})$ that on average $\langle p(\mathbf{r}) \rangle = P_\infty(x)$. Furthermore, site dilution implies that $\mathbf{n}^2(\mathbf{r}) = p(\mathbf{r})$. Thus, on average we have [14] $\langle \mathbf{n}^2(\mathbf{r}) \rangle = P_\infty(x)$. In the continuum limit of (1) the Harris criterion discussed above indicates that in the long-wavelength low-energy limit the magnetic properties of the site diluted problem can be described in terms of an effective QNL σ M:

$$Z = \int D\mathbf{n} \delta[\mathbf{n}^2 - P_\infty(x)] \exp\{-S_{eff}/\hbar\},$$

where

$$S_{eff} = 1/2 \int_0^{\beta\hbar} d\tau \int d\mathbf{r} \left[\chi_\perp(x) |\partial_\tau \mathbf{n}|^2 + \rho_s(x) |\nabla \mathbf{n}|^2 \right] \quad (3)$$

and τ is the imaginary time direction with $\beta = 1/(k_B T)$. Equation (3) leads to a natural description of the undoped system and provides an effective field theory for the QNL σ M in the presence of impurities. Moreover, it

has incorporated the correct properties of the classical percolation problem added to the quantum fluctuations of the QHAF. It is very simple to show by a change of variables that the action in (3) can be rewritten as

$$\frac{S_{eff}}{\hbar} = \frac{1}{2g(x)} \int_0^{\beta\hbar c(x)} d\tau \int d\mathbf{r} (\partial_\mu \mathbf{n})^2 \quad (4)$$

where $g(x) = \hbar c(x)/\rho_s(x)$ is the effective coupling constant of the theory. Moreover, because of the continuum limit the theory has an intrinsic ultraviolet cut-off $\Lambda(x) = 2\sqrt{\pi P_\infty(x)}/a_0$ which is fixed by the total number of states. In writing (4) we have not included the topological term. In a random system one suspects that this term vanishes as in the pure 2D case [15]. Nevertheless there are always statistical fluctuations in a random system which are of order $\sqrt{N_I}$, where N_I is the number of M ions. Thus, the topological term has importance as we discuss at the end of the paper.

The great advantage of (4) is its simplicity and close relationship to the description of the undoped problem. In this paper we use the large N approach for the QNL σ M which has been so successful in describing the undoped system [19]. At zero temperature, a critical value of the coupling constant $g_c(x)$ separates the RC from the QD region. $g_c(x) = 4\pi P_\infty(x)/\Lambda(x)$ can be obtained from the saddle-point equation for (4) [19]. The ratio of the coupling constant to the critical coupling constant is $\bar{g}(x) \equiv g(x)/g_c(x) = \bar{g}_0/P_\infty(x)$, which implies that non-magnetic doping drives the system from RC region to QD region at x_c where $P_\infty(x_c) = \bar{g}_0$ at $T = 0$. The critical concentration x_c is completely determined by the value of \bar{g}_0 in the undoped case. Using the dilute result for $P_\infty(x)$ and $\bar{g}_0 = 0.685$ we find $x_c \approx 0.3$ which is indeed smaller than the percolation threshold $x_p \approx 0.41$ [10]. This result has to be contrasted with classical calculations [20] where long range order is lost at percolation threshold only. We also performed a one-loop renormalization group analysis and calculated the zero temperature staggered magnetization [21] $M_s(x) = M_0(x)\sqrt{1 - \bar{g}(x)}$. Here $M_0(x)$ is the classical staggered magnetization for the perfect Néel spin alignment and the remaining factor is due to quantum fluctuations. Thus, the local average magnetic moment is given by

$$\frac{\langle \mu(x) \rangle}{\langle \mu(0) \rangle} = \frac{M_s(x)/M_0(x)}{M_s(0)/M_0(0)} = \sqrt{\frac{1 - \bar{g}(x)}{1 - \bar{g}(0)}}. \quad (5)$$

Observe that the average local moment indeed vanishes at x_c . For the undoped case, (5) predicts that the maximum measured magnetic moment of Cu ion is $0.56\mu_B$ which agrees with the measured value $0.6 \pm 0.15\mu_B$ [22]. It is also in good agreement with the existing experimental sublattice magnetization measured by μ SR for various doping concentrations as shown in Fig. 1. Notice that for the Ising magnet $\mu(x)$ only deviates from $\mu(0)$ at x_p . The larger reduction of the moment in the QHAF is due to quantum fluctuations present in the QNL σ M.

The magnetic correlation length ξ can be directly calculated from the QNL σ M. The interpolation formula from the RC to the QC region reads [21,23]

$$\xi(x, T) = \left(\frac{e\hbar c(x)}{4} \right) \frac{\exp(2\pi\rho_{R,s}(x)/k_B T)}{4\pi\rho_{R,s}(x) + k_B T}, \quad (6)$$

where $\rho_{R,s}(x) = \rho_s(x)[1 - \bar{g}(x)]$ is the renormalized spin stiffness. This result agrees very well with the Monte Carlo simulations in a large temperature range in the undoped case [24]. As far as we know the only existing neutron scattering results for magnetic correlation length are for the pure system and $x = 0.05$ [16]. In Fig. 2 we plot the available data and the prediction of our model given in (6). As it is well known, samples with $x = 0.05$ have problems with the Oxygen stoichiometry [16]. Excess O introduces mobile holes in the plane which produce strong frustration effects which are not accounted for in our theory. Thus, direct comparison between the theory and experiment for this sample is problematic, especially at high temperatures. Thus, only new experiments with controlled O content can directly test our theory.

Chakravarty and Orbach [25] have calculated the nuclear spin-lattice relaxation rate of Cu for La₂CuO₄ using the dynamical structure factor from the QNL σ M. A detailed calculation was done in Refs. [18,26]. These calculation can be easily extended for the doped case. Here we just quote the result for $\Lambda\xi \gg 1$:

$$\begin{aligned} \frac{1}{T_1(x, T)} &= \gamma^2 P_\infty(x) \sqrt{2\pi^3} S(S+1) \\ &\times \epsilon(A_\perp - 4P_\infty(x)B) \sqrt{1 - \frac{2A_\perp B}{A_\perp^2 + 4B^2}} \\ &\times \frac{[(A_\perp - 4P_\infty(x)B)\xi^2 + 4P_\infty(x)Ba_0^2 \ln(\xi\Lambda)]}{3\omega_e(x)\xi a_0 (\ln(\xi\Lambda))^2} \end{aligned}$$

where γ is the nuclear gyromagnetic ratio, $A_\perp = 80$ kG and $B = 83$ kG are the hyperfine constants [18], and

$$\omega_e(x) = A(x) \sqrt{\left(\frac{2J^2 k_B^2 z S(S+1)}{3\hbar^2} \right)}$$

(where z is the number of nearest neighbor spins) is the corrected Heisenberg exchange frequency. Fig. 3 shows the NMR relaxation rate normalized to the high temperature value as given by the experimental data and the result of our calculations. The growth of the relaxation rate at low temperatures is due to fast growth of ξ . As the system approaches the QCP one starts to see the crossover from RC to the QC regime where the ξ grows like $1/T$ leading to slower growth of the relaxation rate. This behavior is clearly seen in the data since for $x = 0.11$ where growth is very slow from 800K down to 400K. The agreement between data and theory is again quite reasonable.

The 3D Néel order can be obtained from the weak interplane coupling J_\perp and it is given by [1,21,27]:

$$k_B T_N \simeq J_\perp P_\infty(x) \left(\frac{\xi(x, T_N)}{a_0} \right)^2 \left(\frac{M_s(x)}{M_0(x)} \right)^2 \quad (7)$$

which is a transcendental equation for $T_N(x)$. The interplanar coupling constant is insensitive [28] to doping because the change in lattice parameters is negligible [29]. In the undoped case the Néel temperature $T_N(0)$ is of order of 315 K. The initial suppression rate of the Néel temperature with doping, $I = -d \ln(T_N(x))/dx$, when $x \rightarrow 0$ can be directly obtained from (7) and, due to quantum fluctuations it is much faster than in the Ising case (dashed line on Fig.4). We find $I \approx 4.7$ in good agreement with the data. Indeed, in Fig. 4 we show our theoretical results in comparison with various different experimental measurements. The critical concentration x_c for which the system loses long-range order by moving from the RC region to the QD region is approximately 0.305, in agreement with the loss of long-range order at zero temperature as given in (5). Finally, it is also easy to show using the procedure given in ref. [30] that the topological term will lead to induced moments close to the impurities. These moments interact through a random magnetic exchange of order $J e^{-(a_0 x)/\xi(x, T)}$. This effect can lead to order of the induced moments in the paramagnetic phase, as seen experimentally [31,32].

In conclusion, we have proposed an effective QNL σ M to describe the magnetic diluted QHAF. Our model combines the result of classical percolation theory and the quantum fluctuations of the Heisenberg model. Although our model is fairly simple it gives a good quantitative description of the magnetism in La₂Cu_{1-x}M_xO₄. The success of our model in describing the physics of the RC regime is due to the fact that the 2D correlations are very long at finite temperatures and the effect of disorder in the critical behavior is rather weak. Disorder induces quantum fluctuations in the system which lead to the final destruction of LRO at x_c . This effect is not found in classical magnets where LRO is solely determined by the percolation problem. Finally, our arguments indicate that a new approach is required in the QC and QD regions where the NL σ M is probably not applicable.

We thank J. Baez, W. Beyermann, F. Borsa, B. Büchner, P. Carreta, G. Castilla, A. Chernyshev, M. Greven, P. C. Hammel, B. Keimer, D. MacLaughlin, U. Mohideen, and S. Sachdev for useful discussions and comments. We thank P. Carreta for providing us with his experimental results. We also acknowledge support by the A. P. Sloan foundation and support provided by the DOE for research at Los Alamos National Laboratory.

[1] S. Chakravarty *et al.*, Phys. Rev. Lett. **60**, 1057 (1988); Phys. Rev. B **39**, 2344 (1989).

- [2] A. Chubukov *et al.*, Phys. Rev. B **49**, 11919 (1994).
 [3] R. B. Stinchcombe in *Phase Transitions*, Vol. 7 (Academic Press, London, 1983),pg. 151.
 [4] S. Ting *et al.*, Phys. Rev. B **46**, 11772 (1992); E. Manousakis, Phys. Rev. B **45**, 7570 (1992).
 [5] K. B. Lyon *et al.*, Phys. Rev. B **37**, 2353 (1988).
 [6] P. Carretta *et al.*, Isis Ann. Rep. A 524 (1996).
 [7] C. C. Wan *et al.*, Phys. Rev. B **48**, 1036 (1993).
 [8] Y. C. Chen *et al.*, unpublished.
 [9] A. B. Harris, J. Phys. C **7**, 1671 (1974).
 [10] D. Stauffer, *Introduction to Percolation Theory* (Taylor & Francis, London, 1985).
 [11] A. B. Harris and S. Kirkpatrick, Phys. Rev. B **16**, 542 (1977).
 [12] B. P. Watson and P. L. Leath, Phys. Rev. B **9**, 4893 (1974).
 [13] P. C. Hohenberg and B. I. Haperin, Rev. Mod. Phys. **49**, 435 (1977).
 [14] T. Yanagisawa, Phys. Rev. Lett. **68**, 1026 (1992).
 [15] E. Fradkin and M. Stone, Phys. Rev. B **38**, 7215 (1988).
 [16] B. Keimer *et al.*, Phys. Rev. B **46**,14034 (1992); R. J. Birgeneau *et al.*, J. Phys. Chem. Solid **56**, 1913 (1995); B. Keimer, Ph. D. Thesis (MIT, 1991).
 [17] M. Matsumura *et al.*, J. Phys. Soc. Jpn. **63**,4331 (1994).
 [18] P. Carretta *et al.*, Phys. Rev. B **55**, 3734 (1997); M. Corti *et al.*, Phys. Rev. B **52**, 4226 (1995).
 [19] S. Sachdev, in *Low-Dimensional Quantum Field Theories for Condensed Matter Physicists*, Proc. of the Trieste Summer School (World Scientific, Singapore, 1992).
 [20] G. S. Rushbrooke and D. J. Morgan, Mol. Phys. **4**, 1 (1961).
 [21] A. H. Castro Neto and D. Hone, Phys. Rev. Lett. **76**, 2165 (1996).
 [22] D. Vaknin *et al.*, Phys. Rev. Lett. **58**, 2802 (1987).
 [23] P. Hasenfratz and F. Niedermayer, Phys. Lett. B **268**, 231 (1991).
 [24] B. B. Beard *et al.*, Phys. Rev. Lett. **80**, 1742 (1998).
 [25] S. Chakravarty and R. Orbach, Phys. Rev. Lett. **64**, 224 (1990).
 [26] T. Imai *et al.*, Phys. Rev. Lett. **70**, 1002 (1993).
 [27] D. Hone and A. H. Castro Neto, Journal of Superconductivity **10**, 349 (1997).
 [28] A. Chakraborty *et al.*, Phys. Rev. B **40**, 5296 (1989).
 [29] K. Uchinokura *et al.*, Physica B **205**, 234 (1995).
 [30] N. Nagaosa *et al.*, J. Phys. Soc. Jpn. **65**, 3724 (1996).
 [31] M. Hücker *et al.*, Phys. Rev. B **59**, R725 (1999).
 [32] P. Mendels *et al.*, Phys. Rev. B **49**, 10035 (1994).
 [33] S-W. Cheong *et al.*, Phys. Rev. B **44**, 9739 (1991).

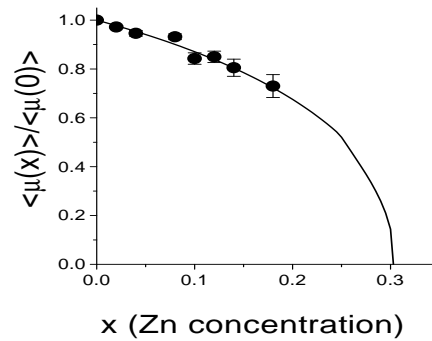


FIG. 1. Effective moment at $T = 0$ as function of x (normalized relative to the undoped case) and the experimental data for $\text{La}_{2-x}\text{Zn}_x\text{O}_4$ [6].

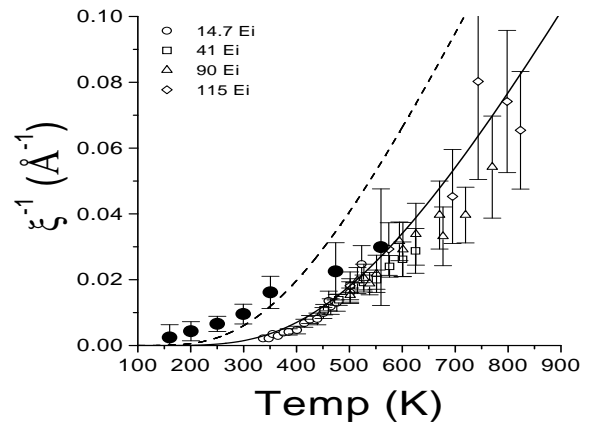


FIG. 2. Inverse correlation length as function of temperature for $x = 0$ (solid line) and $x = 0.05$ (dashed line). The open ($x = 0$) and solid symbols ($x = 0.05$) are the neutron scattering data [16].

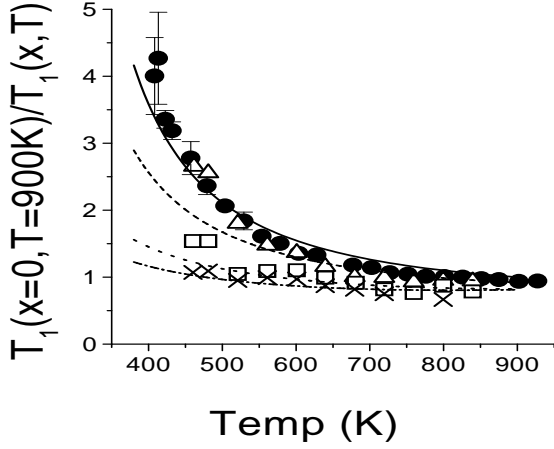


FIG. 3. The Cu $1/T_1$ normalized to the undoped case at high temperatures ($T = 900$ K). The lines from top to bottom are for $x = 0$ (solid), $x = 0.025$ (long dash), $x = 0.08$ (short dash), and $x = 0.11$ (dotted dash). $x = 0$ (solid circles - NQR data [17]) and $x = 0.025$ (open triangle), $x = 0.08$ (open square) $x = 0.11$ (cross) (NQR data [18]).

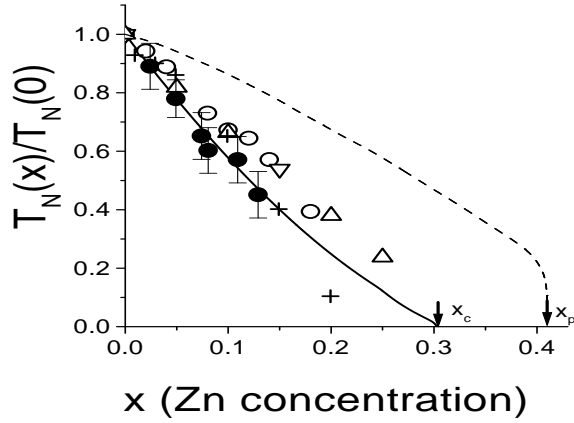


FIG. 4. Néel temperature normalized to the undoped case. Solid line: 7; dashed line: Ising result. Experimental data for $\text{La}_2\text{Cu}_{1-x}\text{Zn}_x\text{O}_4$: Solid and open circles are NQR and μSR data, respectively [18]; straight and up-side-down triangles are magnetic susceptibility data [31]; crosses are magnetization data [33].